



NINE LEVEL INVERTER DESING WITH PV INPUT

¹NallamelliPremTeja, ²M. Praveen

¹PG Student, ²Assistant Professor, EEE Dept.

GITAM Institute of Technology, Rushikonda

Visakhapatnam, India

Email: ¹Premteja.222@gmail.com, ²praveenmande@gmail.com

Abstract—A single-phase grid-connected inverter is usually used for residential or low-power applications of power ranges that are less than 10 kW. Types of single-phase grid-connected inverters have been investigated. The three-level inverter can satisfy specifications through its very high switching, but it could also unfortunately increase switching losses, acoustic noise, and level of interference to other equipment. Improving its output waveform reduces its harmonic content and, hence also the size of the filter used and the level of electromagnetic interference (EMI) generated by the inverter's switching operation. In this paper a single-phase seven-level inverter for grid-connected photovoltaic systems, with a novel pulse width-modulated (PWM) control scheme is designed. Three reference signals that are identical to each other with an offset that is equivalent to the amplitude of the triangular carrier signal were used to generate the PWM signals. The inverter is capable of producing seven levels of output-voltage levels (V_{dc} , $2V_{dc}/3$, $V_{dc}/3$, 0 , $-V_{dc}/3$, $-2V_{dc}/3$, $-V_{dc}$) from the dc supply voltage. Multilevel inverters offer improved output waveforms and lower THD. The behavior of the proposed multilevel inverter was analyzed in detail by using MATLAB. The results obtained from 7-level inverter are compared with 9 level by using a separate control.

IndexTerms—FACTS device, State Estimation, UPFC, PMU.

I. INTRODUCTION

The ever-increasing energy consumption, fossil fuels' soaring costs and exhaustible nature, and worsening global environment have created a booming interest in renewable energy generation systems, one of which is photovoltaic. Such a system generates electricity by converting the Sun's energy directly into electricity. Photovoltaic-generated energy can be delivered to power system networks through grid-connected inverters. A single-phase grid-connected inverter is usually used for residential or low-power applications of power ranges that are less than 10 kW. Types of single-phase grid-connected inverters have been investigated. A common topology of this inverter is full-bridge three-level. The three-level inverter can satisfy specifications through its very high switching, but it could also unfortunately increase switching losses, acoustic noise, and level of interference to other equipment. Improving its output waveform reduces its harmonic content and, hence, also the size of the filter used and the level of electromagnetic interference (EMI) generated by the inverter's switching operation. Multilevel inverters are promising; they have nearly sinusoidal output-voltage waveforms, output current with better harmonic profile, less stressing of electronic components owing to decreased voltages, switching losses that are

lower than those of conventional two-level inverters, a smaller filter size, and lower EMI, all of which make them cheaper, lighter, and more compact. Various topologies for multilevel inverters have been proposed over the years. Common ones are diode-clamped, flying capacitor or multi cell, cascaded H-bridge and modified H-bridge multi level. This paper recounts the development of a novel modified H-bridge single-phase multilevel inverter that has two diode embedded bidirectional switches and a novel pulse width modulated (PWM) technique. The topology was applied to a grid-connected photovoltaic system with considerations for a maximum-power-point tracker (MPPT) and a current-control algorithm. By using MPPT the maximum power point will be obtained and the simulated results are explained.

II. PHOTOVOLTAIC SYSTEM

2.1 Photovoltaic Effect

Photovoltaic (PV) is a method of generating electrical power by converting solar radiation into direct current electricity using semiconductors that exhibit the photovoltaic effect. Photovoltaic power generation employs solar panels comprising a number of cells containing a photovoltaic material. Materials presently used for photovoltaic include mono crystalline silicon, polycrystalline silicon, amorphous silicon, cadmium telluride and copper indium selenide/sulfide. Due to the growing demand for renewable energy sources, the manufacturing of solar cells and photovoltaic arrays has advanced considerably in recent years.

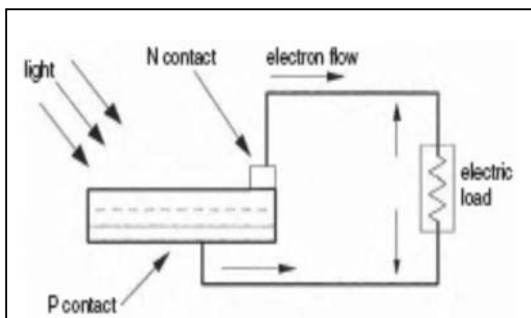


Fig 2.1: PV effect converts the photon energy into voltage across the p-n junction

2.2 Equivalent Circuit

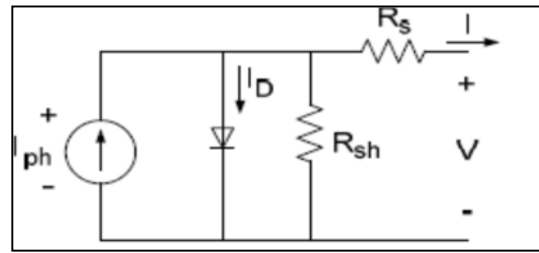


Fig 2.2 PV cell equivalent circuit

The complex physics of the PV cell can be represented by the equivalent electrical circuit. The circuit parameters are as follows. The series resistance R_s represents the internal resistance to the current flow, and depends on the pn-junction depth, impurities, and contact resistance. The shunt resistance R_{sh} is inversely related to the leakage current to ground. In an ideal PV cell, $R_s = 0\Omega$ (no series loss) and $R_{sh} = \infty$ (no leakage to ground). In a typical high-quality silicon cell, R_s varies from 0.05 to 0.10 Ω and R_{sh} from 200 to 300 Ω . The PV conversion efficiency is sensitive to small variations in R_s , but is insensitive to variations in R_{sh} . A small increase in R_s can decrease the PV output significantly. In the equivalent circuit, the current delivered to the external load equals the current I_{ph} generated by the illumination, less the diode current I_D and the shunt leakage current I_{sh} . The open-circuit voltage V_{oc} of the cell is obtained when the load current is zero, i.e., when $I = 0$, and is given by the following:

$$V_{oc} = V + IR_{sh}$$

The shunt resistance (R_{sh}) is very large and the series resistance (R_s) is very small. Therefore, it is common to neglect these resistances in order to simplify the solar cell model. The resultant ideal voltage-current characteristic of a photovoltaic cell is given by the relation below and illustrated by the figure above.

$$I = I_{ph} - I_D$$

$$I = I_{ph} - I_0$$

Where,

I_{ph} = photocurrent,

I_D = diode current,

I_0 = saturation current,

A = ideality factor,

q = electronic charge 1.6×10^{-19} ,

k_B = Boltzmann's gas constant (1.38×10^{-23}),

T = cell temperature,

R_s = series resistance,

R_{sh} = shunt resistance,

I = cell current,
 V = cell voltage
 The power output of a solar cell is given by
 $P_{PV} = V_{PV} * I_{PV}$
 Where,
 I_{PV} = Output current of solar cell (A).
 V_{PV} = Solar cell operating voltage (V).
 P_{PV} = Output power of solar cell (W).

2.3 MPPT (Maximum Power Point Tracking)

Maximum power point

Is the operating point A (V_{max} , I_{max}) at which the power dissipated in the resistive load is maximum: $P_{max} = I_{max} * V_{max}$

Maximum efficiency

Is the ratio between the maximum power and the incident light power. In current practice, the performance of a module or another PV device is determined by exposing it at known conditions. The module characteristics supplied by the manufacturer are usually determined under special conditions. The operating point A (V_{max} , I_{max}) at which the power dissipated in the resistive load is maximum. $P_{max} = I_{max} * V_{max}$. The maximum value for the MPPT is 1000wb/m² at this point of instant the maximum power will be collected by the MPPT. By using this we can improve the efficiency and output response of the photovoltaic cell (PV).

2.3.1 MPPT Algorithms

Maximum power point trackers may implement different algorithms and switch between them based on the operating conditions of the array. The various MPPT algorithms or methods are,

1. Constant Voltage
2. Short Circuit Current
3. Incremental Conductance
4. Perturb and Observe

2.3.2 Proposed MPPT Algorithm

The proposed MPPT algorithm is Perturb and Observe with current being controlled. Generally, the designer has a choice of either changing the PV voltage or current. Fig 2.3 shows that changes in V_{MP} are closely related to $\ln(\text{irradiance})$ and Fig 2.4 shows that I_{MP} is proportional to irradiance.

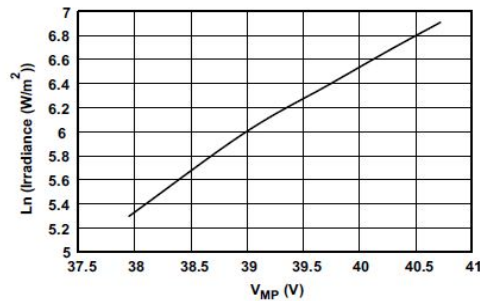


Figure 2.3 Irradiance vs V_{MP} for 200 to 1000 W/m²

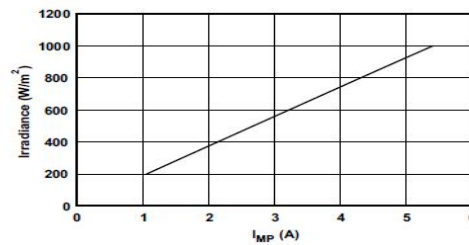


Figure 2.4 Irradiance vs I_{MP} for 200 to 1000 W/m²

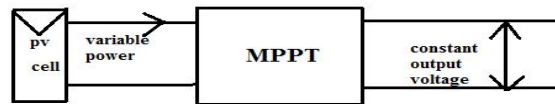


Fig 2.6 Block diagram of P&O Algorithm

III. STEP-UP CHOPPER/ BOOST CHOPPER

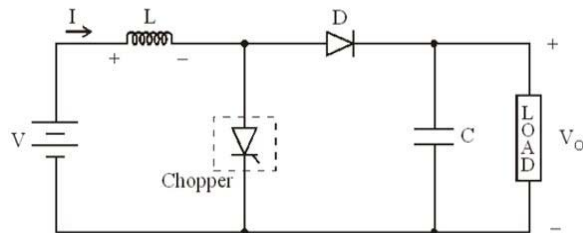


Fig 3.1 Step-Up Chopper/Boost Chopper

Figure 3.1 shows a step-up chopper to obtain a load voltage V_o higher than the input voltage V . the values of L and C are chosen depending upon the requirement of output voltage and current. When the chopper is ON, the inductor L is connected across the supply. The inductor current ' I ' rises and the inductor stores energy during the ON tie of chopper, T_{on} . When the chopper is off, the inductor current I is forced to flow through the diode D and load for a period, T_{off} . The current tends to decrease resulting in

reversing the polarity of induced EMF in L. therefore voltage across load is given by

$$V_o = V + L \frac{di}{dt} \text{ i.e., } V_o > V$$

The thyristor in the circuit acts as a switch. When thyristor is ON, supply voltage appears across the load and when thyristor is OFF, the voltage across the load will be zero. The above circuit depicts a step-up or a PWM boost converter. It consists of dc input voltage source V_s , boost inductor L, controlled switch S, diode D, filter capacitor C, and load resistance R. The converter waveforms in the CCM are presented in Fig below. When the switch S is in the on state, the current in the boost inductor increases linearly and the diode D is off at that time. When the switch S is turned off, the energy stored in the inductor is released through the diode to the particular load (R-Load).

IV. INVERTERS

4.1 Introduction to Inverters

D.C.-A.C. inverters are electronic devices used to produce mains voltage A.C. power from low voltage D.C. energy (from a battery or solar panel). This makes them very suitable for when you need to use A.C. power tools or appliances but the usual A.C. mains power is not available. Examples include operating appliances in caravans and mobile homes, and also running audio, video and computing equipment in remote areas. Most inverters do their job by performing two main functions: first they convert the incoming D.C. into A.C., and then they step up the resulting A.C. to mains voltage level using a transformer. And the goal of the designer is to have the inverter perform these functions as efficiently as possible so that as much as possible of the energy drawn from the battery or solar panel is converted into mains voltage A.C., and as little as possible is wasted as heat.

4.2 Proposed Multilevel Inverter Topology

The proposed single-phase seven-level inverter was developed from the five-level inverter. It comprises a single-phase conventional H-bridge inverter, two bidirectional switches, and a capacitor voltage divider formed by C_1 , C_2 , and C_3 . The modified H-bridge topology is significantly advantageous over other topologies, i.e., less power switch, power diodes, and less capacitors for inverters of the same number of levels. Photovoltaic (PV) arrays were

connected to the inverter via a dc–dc boost converter. The power generated by the inverter is to be delivered to the power network, so the utility grid, rather than a load, was used. The DC–DC boost converter was required because the PV arrays had a voltage that was lower than the grid voltage. High dc bus voltages are necessary to ensure that power flows from the PV arrays to the grid. A filtering inductance L_f was used to filter the current injected into the grid. Proper switching of the inverter can produce seven output-voltage levels (V_{dc} , $2V_{dc}/3$, $V_{dc}/3$, 0 , $-V_{dc}$, $-2V_{dc}/3$, $-V_{dc}/3$) from the dc supply voltage. The proposed inverter’s operation can be divided into seven switching states, as shown in Fig. 4.1 – 4.7.

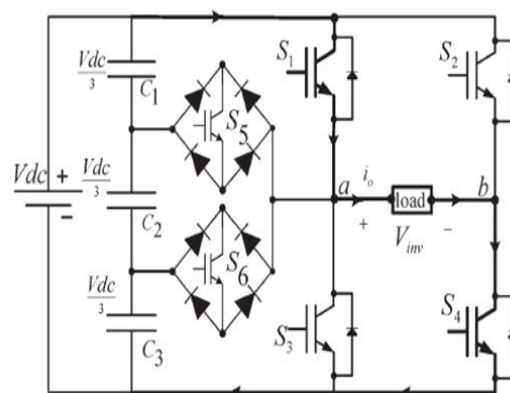


Fig 4.1 Inverter circuit for the output voltage (V_{dc})

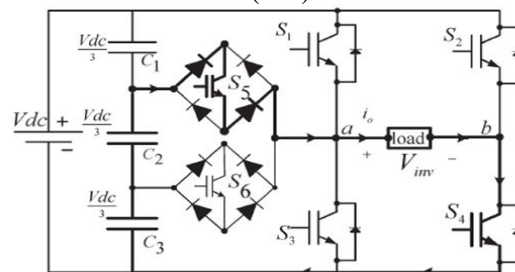


Fig 4.2 Inverter circuit for the output voltage ($2V_{dc}/3$)

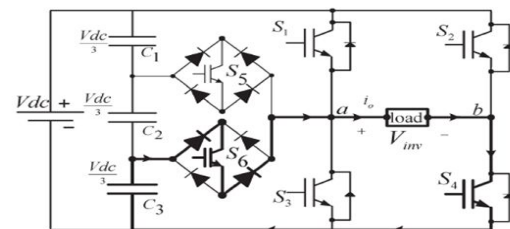


Fig 4.3 Inverter circuit for the output voltage ($V_{dc}/3$)

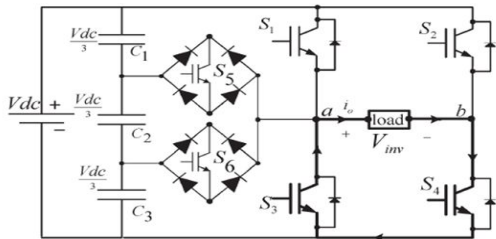


Fig 4.4 Inverter circuit for the output voltage (zero 0)

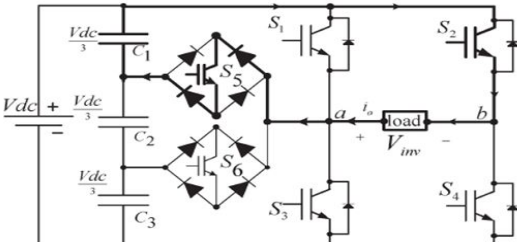


Fig 4.5 Inverter circuit for the output voltage (-V_{dc}/3)

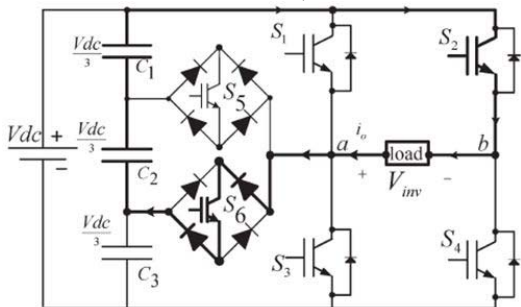


Fig 4.6 Inverter circuit for the output voltage (-2V_{dc}/3)

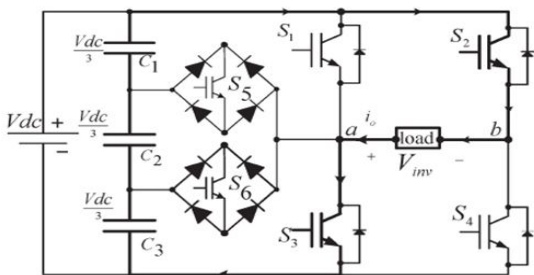


Fig 4.7 Inverter circuit for the output voltage (-V_{dc})

Table 4.1 Output voltage according to the switches on-off condition

v_0	S_1	S_2	S_3	S_4	S_5	S_6
V_{dc}	on	off	off	on	off	off
$2V_{dc}/3$	off	off	off	on	on	off
$V_{dc}/3$	off	off	off	on	off	on
0	off	off	on	on	off	off
0*	on	on	off	off	off	off
$-V_{dc}/3$	off	on	off	off	on	off
$-2V_{dc}/3$	off	on	off	off	off	on
$-V_{dc}$	off	on	on	off	off	off

Table shows the switching combinations that generated the seven output-voltage levels ($0, -V_{dc}, -2V_{dc}/3, -V_{dc}/3, V_{dc}, 2V_{dc}/3, V_{dc}/3$).

V. CONTROL STRATEGY

5.1 Introduction

As Fig. 5.1 shows, the control system comprises a MPPT algorithm, a dc-bus voltage controller, reference-current generation, and a current controller. The two main tasks of the control system are maximization of the energy transferred from the PV arrays to the grid, and generation of a sinusoidal current with minimum harmonic distortion, also under the presence of grid voltage harmonics. The proposed inverter utilizes the perturb-and-observe (P&O) algorithm for its wide usage in MPPT owing to its simple structure and requirement of only a few measured parameters. It periodically perturbs (i.e., increment or decrement) the array terminal voltage and compares the PV output power with that of the previous perturbation cycle. If the power was increasing, the perturbation would continue in the same direction in the next cycle; otherwise, the direction would be reversed. This means that the array terminal voltage is perturbed every MPPT cycle; therefore, when the MPP is reached, the P&O algorithm will oscillate around it. The P&O algorithm was implemented in the dc–dc boost converter. The output of the MPPT is the duty-cycle function. As the dc-link voltage V_{dc} was controlled in the AC-DC seven level PWM inverter, the change of the duty cycle changes the voltage at the output of the PV panels. A PID controller was implemented to keep the output voltage of the DC–DC boost converter (V_{dc}) constant by comparing V_{dc} and V_{dcref} and feeding the error into the PID controller, which subsequently tries to reduce the error. In this way, the V_{dc} can be maintained at a constant value and at more than $\sqrt{2}$ of V_{load} to deliver power to the load. To deliver energy to the grid, the frequency and phase of the PV inverter must equal those of the grid; therefore, a grid synchronization method is needed. The sine lookup table that generates reference current must be brought into phase with the grid voltage (V_{load}). For this, the grid period and phase must be detected. The overall response is controlled under this block and the different PID controllers are used for the generation of the sinusoidal

signal and the sine lookup table and zero crossing detector are used for the sinusoidal signal. The overall response is controlled under the closed loop conditions to get the accurate output.

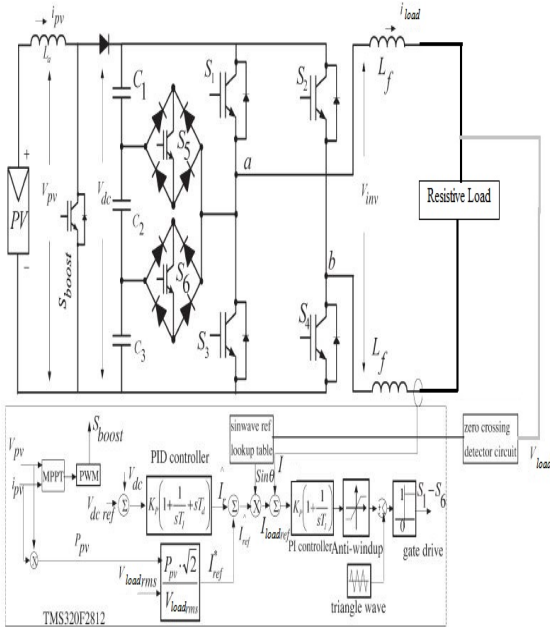


Fig. 5.1 Seven-level inverter with closed-loop control algorithm

VI. SIMULATION RESULTS

6.1 Block Diagrams

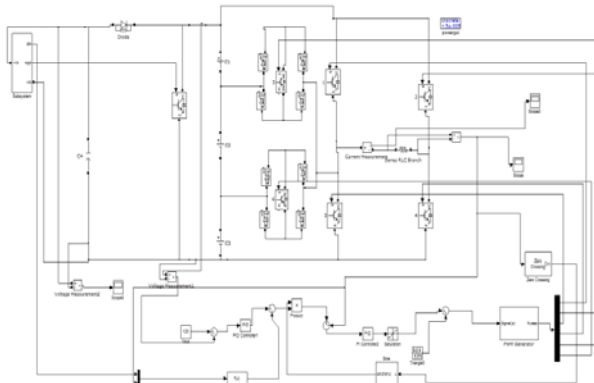


Fig 6.1 Main MATLAB/SimuLink Block diagram

6.2 Simulation Results

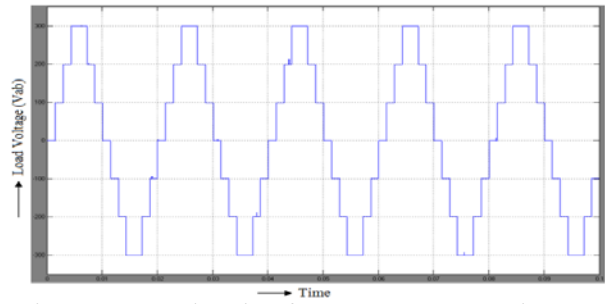


Fig 6.2 Seven levels of Inverter output voltage (V_{inv})

6.3 Nine Level Simulation

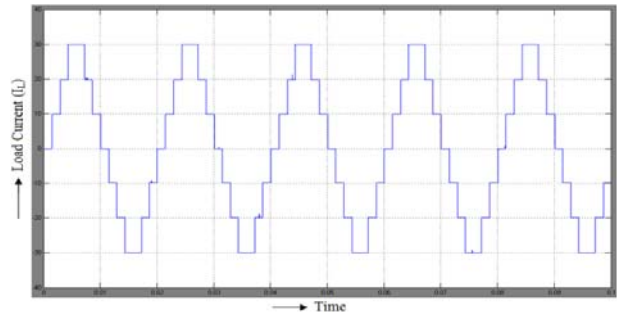


Fig 6.3 Seven levels of Inverter output current (I_{inv})

For $R=10\Omega$

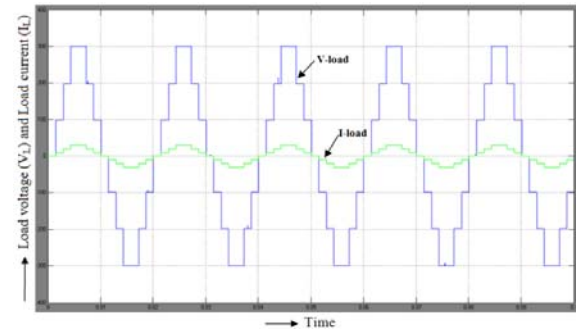


Fig 6.4 Load voltage (V_{Load}) and Load current (I_{Load}) that are in phase

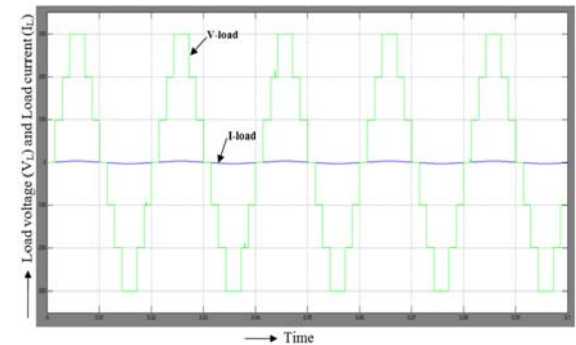


Fig 6.5 Load voltage (V_{Load}) and Load current (I_{Load}) that are in phase

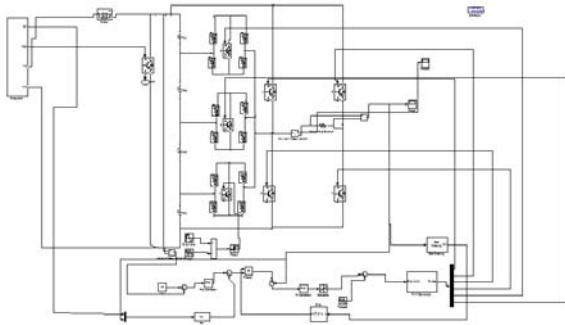


Fig 6.6 Main MATLAB/Simulink Block diagram

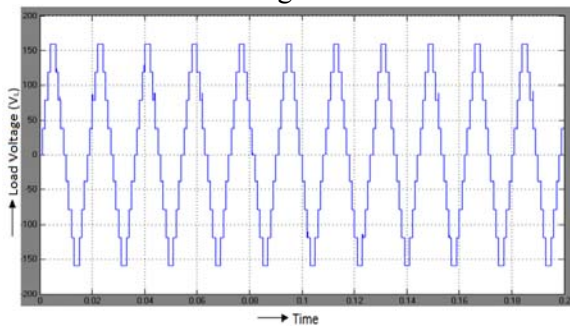


Fig 6.7 Nine levels of Inverter output voltage (V_{inv})

VII. CONCLUSIONS

This paper has presented a novel PWM switching scheme for the proposed multilevel inverter. It utilizes three reference signals and a triangular carrier signal to generate PWM switching signals. The behavior of the proposed multilevel inverter was analyzed in detail. By controlling the modulation index, the desired number of levels of the inverter's output voltage can be achieved. The results obtained are compared with nine level inverter. The less THD in the seven-level inverter is an attractive solution for grid-connected PV inverters. By using this seven level inverter we can improve the overall response of the system with the less number of switching states and the reliable operation. By considering nine level inverter THD can be reduced which is less than the THD obtained from seven level inverter.

REFERENCES

[1] Nasrudin A. Rahim, Jeyraj Selvaraj, "Single-Phase Seven-Level Grid-Connected Inverter for Photovoltaic System", *IEEE Trnas.on industrial electronics*, VOL. 58, NO. 6, JUNE 2011.
 [2] S. B. Kjaer, J. K. Pedersen, and F. Blaabjerg, "A review of single-phase grid connected

inverters for photovoltaic modules," *IEEE Trans. Ind. Appl.*, vol. 41, no. 5, pp. 1292–1306, Sep./Oct. 2005.

[3] J. Rodriguez, J. S. Lai, and F. Z. Peng, "Multilevel inverters: A survey of topologies, controls, and applications," *IEEE Trans. Ind. Electron.*, vol. 49, no. 4, pp. 724–738, Aug. 2002.

[4] J. Selvaraj and N. A. Rahim, "Multilevel inverter for grid-connected PV system employing digital PI controller," *IEEE Trans. Ind. Electron.*, vol. 56, no. 1, pp. 149–158, Jan. 2009.

[5] J. Huang and K. A. Corzine, "Extended operation of flying capacitor multilevel inverter," *IEEE Trans. Power Electron.*, vol. 21, no. 1, pp. 140–147, Jan. 2006.

[6] J. I. Leon, S. Vazquez, S. Kouro, L. G. Franquelo, J. M. Carrasco, and J. Rodriguez, "Unidimensional modulation technique for cascaded multilevel converters," *IEEE Trans. Ind. Electron.*, vol. 49, no. 5, pp. 1058–1064, Oct. 2002.

[7] G. Ceglia, V. Guzman, C. Sanchez, F. Ibanez, J. Walter, and M. I. Gimenez, "A new simplified multilevel inverter topology for DC–AC conversion," *IEEE Trans. Power Electron.*, vol. 21, no. 5, pp. 1311–1319, Sep. 2006.

[8] N. A. Rahim and J. Selvaraj, "Multi-string five-level inverter with novel PWM control scheme for PV application," *IEEE Trans. Ind. Electron.*, vol. 57, no. 6, pp. 2111–2121, Jun. 2010.

[9] E. Villanueva, P. Correa, J. Rodríguez, and M. Pacas, "Control of a single phase cascaded H-bridge multilevel inverter for grid-connected photovoltaic systems," *IEEE Trans. Ind. Electron.*, vol. 56, no. 11, pp. 4399–4406, Nov. 2009.

[10] "Modeling and Simulation of Photovoltaic module using MATLAB/Simulink", *International Journal of Chemical and Environmental Engineering*, Volume 2, No.5, October 2011.

[11] "Mathematical Modeling and Simulation of Photovoltaic Cell using Matlab-Simulink Environment", *International Journal of Electrical and Computer Engineering (IJECE)*, Vol. 2, No. 1, February 2012